Increasing the temperature of inlet water is one way to increase solar distillation efficiency. Heat recovery using double glazing is a more straightforward way to raise the temperature of inlet water. In previous studies, the incoming water temperature was raised using additional equipment such as a solar water heater collector or utilizing the heat of wastewater from another water distillation system. The earlier studies' technique caused solar water distillation to be complicated, and the manufacturing cost was expensive. Heat recovery is a process of utilizing heat condensation of water vapor to increase the inlet water temperature. In conventional solar distillation, condensing heat is not used and wasted into the environment. Double glass is two glasses arranged in parallel, one on the top of the other. The distance between the glasses is 2 mm. The bottom glass is a 1 m^2 distillation cover glass. Water flows between the bottom glass and the top glass before entering the distillation model. The inlet water receives heat condensation so that the temperature rises. The increase in temperature causes heat loss to decrease and leads to efficiency improvement. This study aims to reveal the effect of heat recovery using double glazing to improve solar distillation efficiency. The study was conducted with laboratory experiments and simulations. The thickness of the bottom and top glass and the top glass area influence the heat recovery process. This study used two variations of glass thickness, namely 3 mm and 5 mm. The area of the top glass was varied by 0.1, 0.5, 0.7, and 1.0 m^2. The maximum efficiency improvement compared to distillation without heat recovery obtained is 39.6 % with a glass thickness of 3 mm and 51.0 % with a glass thickness of 5 mm achieved in the variation of the top glass area of 0.1 m^2

Keywords: heat recovery, double glazing, inlet water temperature, efficiency improvement

UDC 620
DOI: 10.15587/1729-4061.2020.209751

INCREASING INLET WATER TEMPERATURE USING CONDENSATION HEAT TO IMPROVE SOLAR DISTILLATION EFFICIENCY

Rusdi Sambada
PhD Student*
Lecturer
Department of Mechanical Engineering
Faculty of Sains and Technology
Sanata Dharma University
Kampus III, Paingan, Maguwoharjo, Depok, Sleman,
Yogyakarta, Indonesia, 55282
E-mail: sambada@usd.ac.id
Sudjito Soeparman
PhD, Professor*
E-mail: sudjitospn@ub.ac.id
Widya Wijayanti
Associate Professor*
E-mail : widya_dinata@ub.ac.id
Eko Siswanto
Associate Professor*
E-mail : eko_s112@ub.ac.id
*Department of Mechanical Engineering
Brawijaya University
Jl. Mayjend Haryono, 167, Malang, Indonesia, 65145

Received date 17.08.2020
Accepted date 12.10.2020
Published date 23.10.2020

1. Introduction

Distillation of water with solar distillation (SS) is an easy and inexpensive way to purify brackish water or seawater to become potable water, especially in remote areas. The inclined SS is a type of SS that is widely used. However, the efficiency of a conventional inclined SS is generally low [1]. SS research is usually carried out to increase efficiency [2]. The critical thing of SS design is that it can minimize heat losses and maximize the trapped heat energy [3].

The more heat energy trapped, the higher the distillation efficiency. The parameters that affect the amount of heat energy trapped are the heating time of the water in the absorber and the temperature of the inlet water [4, 5]. Modifying the shape of the absorber on inclined SS with grooves, fins, baffles, and partitions can increase the heating time of water in the absorber so that the water temperature increases [3]. The author of the paper [6] shows that the use of baffles on inclined SS can increase efficiency by 68 % compared without baffles. In [7], the authors examine the use of partitions, which improve efficiency by 19.76 % compared to conventional inclined SS. Modification of the absorber shape can indeed increase the heating time. However, it takes a longer time for the water in the absorber to reach the evaporation temperature. The longer time for water to reach the evaporation temperature is due to the lower inlet water temperature.

Therefore, studies are devoted to finding a method to increase the temperature of the input water effectively. The increase in the inlet water temperature caused the distillation model's water to reach the evaporation temperature faster. The faster the inlet water achieves the evaporation temperature, the higher the distillation efficiency. Nowadays, solar water distillation is generally used in remote areas. Therefore, increasing the temperature of the incoming

water must be effective and easy to manufacture, use, maintain, and low-cost.

2. Literature review and problem statement

As explained above, the inlet water temperature is one of the parameters that affect the amount of heat energy trapped. The higher the temperature of the inlet water, the more heat energy is trapped. Some studies use other systems to increase the inlet water temperature of SS. In [8], the author researched the use of solar water heater collectors to raise the temperature of the inlet water, which increased production by 36 %. However, the main problem that arises with the use of solar water heater collectors is cost. It takes a lot of additional costs for the manufacture or purchase of a solar water heater collector. In [9], the author combines the humidification-dehumidification (HDH) system with six inclined SS. Inlet water for SS is hot water that comes from the HDH system. The production of HDH and inclined SS systems has increased compared to HDH systems alone. The author of [10] uses HDH wastewater as inlet water into the inclined SS. Increased efficiency compared to basin type SS was 210.2 %. However, not all places where solar water distillation will be applied have HDH systems already installed. Often the application of solar energy water distillation is in remote areas, where there is no other system that can be used to increase the efficiency of solar energy water distillation. In the inclined SS, there is some loss of heat energy, one of which is the heat loss on the exit side. The loss of heat on the exit side is caused by the water that does not evaporate and comes out as hot wastewater. Some studies utilize heat losses on this side to increase the inlet water temperature. In the paper [11] and [12], the authors use wastewater that comes out of inclined SS as inlet water in basin type SS. Increased efficiency obtained was 46.23 % [11] and 25.75 % [12] compared to conventional basin SS. Utilizing heat loss from one system to increase the efficiency of other solar water distillation is a cheaper method than using a solar water heater collector. This method is also simpler than using the HDH system. However, this method still has technical problems. The use of two different types of solar water distillation systems creates issues related to the regulation of the inlet water flow, which is quite complicated. In the paper [13], the author circulated the inclined SS's wastewater as inlet water using a pump, which resulted in the increased efficiency by 57.2 % compared to basin SS obtained by simulation. The utilization of wastewater as input water in the inclined SS in the paper [13] is an appropriate way to raise the temperature of the inlet water. However, using a water pump to flow the wastewater to the inlet is a drawback of this method. Using a pump adds to the cost and complexity of controlling the flow rate. Another problem is the need for electricity for pumps, which must be provided by the solar cell system, especially in remote areas where there is no electricity. The most important thing from the design of an SS is that it is easy to make and operate, and also efficient in producing clean water [14]. The use of other systems or wastewater from heat losses on the exit side to raise the inlet water temperature causes the design of the SS to become complicated. All this suggests that it is advisable to conduct a study on a cheap and straightforward method to raise the temperature of the inlet water. This study proposes a new method that is easier and simpler to increase the inlet water temperature. The new method is heat recovery using double glazing (Fig. 1). Heat recovery is the use of heat losses on the top side of the distillation to heat the inlet water. In a conventional inclined SS, the heat loss on the top side comes from the heat energy released by water vapor during the condensation process on the cover glass inner surface. In a conventional inclined SS, the condensing heat energy is released into the environment through the glass cover without being utilized.

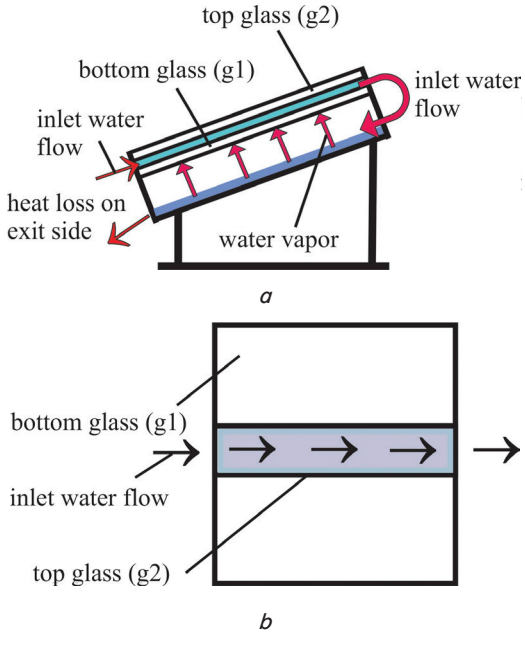

Fig. 1. Heat recovery using double glass: *a* — side view; *b* — top view

Double glass is two glasses arranged in parallel, one on the top of the other. The distance between the glasses is 2 mm. The bottom glass is a 1 m^2 distillation cover glass. Inlet water flows between the bottom glass (g_1) and the top glass (g_2) before entering the distillation model. While flowing, the inlet water receives heat condensation so that the temperature rises (Fig. 1). The thickness of the bottom and top glasses and the area of the upper glass are factors that influence the heat recovery process. This study used two variations of glass thickness. The variation of the area of the upper glass is expressed as the ratio of the area of the top glass to the area of the bottom glass (A_{g2}/A_{g1}).

However, there has been no previous research regarding condensation heat to increase solar water distillation inlet water temperature. Therefore, research needs to be carried out to determine the increase in the inlet water temperature that can be achieved, the reduction in heat energy loss that occurs, the increase in efficiency that can be achieved, and the Ag_2/Ag_1 ratio, which results in the maximum efficiency increase.

3. The aim and objectives of the study

The study aims to determine the maximum efficiency improvement of solar energy water distillation due to the utilization of condensation heat (heat recovery) for increasing inlet water temperature. A distillation model without a heat recovery (SG) model was used as a comparison of the distillation model with heat recovery (DG) models.

To achieve this aim, the following objectives are accomplished:

– by determining the increase of the inlet water temperature of the DG model compared to the SG model distillation;

– by calculating the reduction of heat energy losses at the inlet side and exit side of the DG model compared to the SG model;

– by calculating the efficiency improvement of the DG model compared to the SG model using a 3 mm and 5 mm thick cover glass;

– by determining the variation of A_{g2}/A_{g1}, which yields the maximum efficiency improvement of the DG model.

4. Materials and methods

4. 1. Model description

The DG model scheme is shown in Fig. 2. The main parts of DG are the top glass (g_2), the bottom glass (g_1), the absorber (b), and the outer frame. This study uses two variations in the thickness of the top glass (g_2) and the bottom glass (g_1), i. e. 3 mm and 5 mm. The area of the bottom glass (g_1) of the DG model is 1 m^2. The area of the top glass (g_2) of the DG model varied by 0.1, 0.5, 0.7, and 1 m^2. In other words, the area ratio of the top and bottom glasses (A_{g2}/A_{g1}) of the DG model is varied by 0.1, 0.5, 0.7, and 1.0 (Fig. 3).

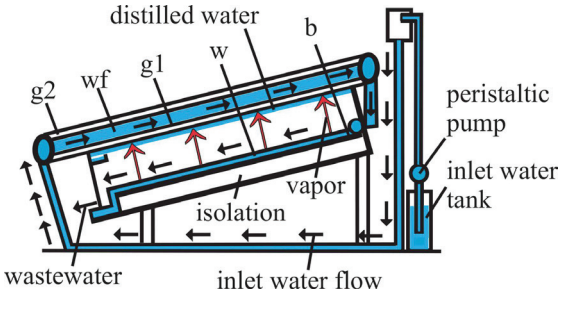

Fig. 2. Scheme of the DG model (side view)

Wick absorber has a thickness of 1.5 mm and is black. The size of the outer frame is 1.35×0.9 m. Insulation is made of glass fiber insulation material with a thermal conductivity value of 0.043 W/m·°C. Insulation thickness is 5 cm. DG has a length of 1.25 m, width of 0.8 m. The slope of the DG is 15°. The absorbance of the wick is 0.9. The absorbance and the reflectivity of the 3 mm thick cover glass are 0.09 and 0.05, respectively. The absorbance and the reflectivity of the 5 mm thick cover glass are 0.19 and 0.17, respectively. The distance between the top glass (g_2) and the bottom glass (g_1) on the DG model is 2 mm.

The inlet water of DG (w_f) flows through the gap between the top glass (g_2) and the bottom glass (g_1). The inlet water flows from the lower side to the upper side of the cover glass, then enters the absorber (Fig. 2, 3). The SG model scheme is shown in (Fig. 4, 5).

The main parts of the SG model are the same as the DG model except for the absence of the top glass (g_2). The SG model only has one cover glass (g_1), or the SG model is distillation with A_{g2}/A_{g1} of 0.0. In other words, the SG model is a distillation model without heat recovery and is used as a comparison of the distillation model with heat recovery (DG model). Inlet water of SG (w) flows directly from the inlet water tank to the upper side of the absorber and flows to the lower side of the absorber (Fig. 4). In this study, the inlet water flow rate of both SG and DG models is 3.5 kg/hour.

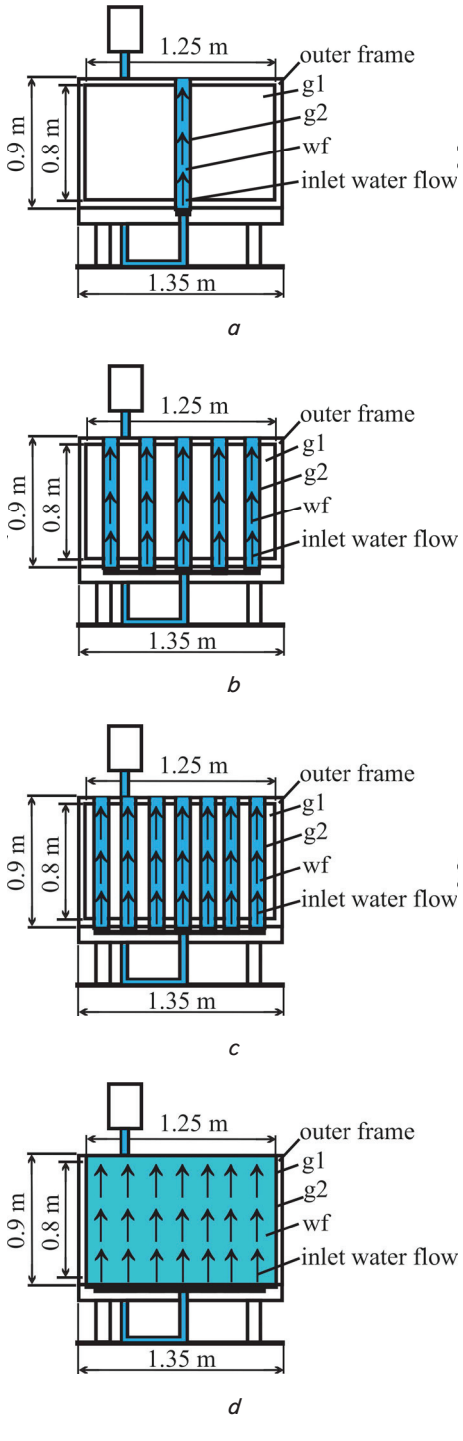

Fig. 3. Scheme of DG (front view): a – A_{g2}/A_{g1}=0.1, b – A_{g2}/A_{g1}=0.5, c – A_{g2}/A_{g1}=0.7, d – A_{g2}/A_{g1}=1.0

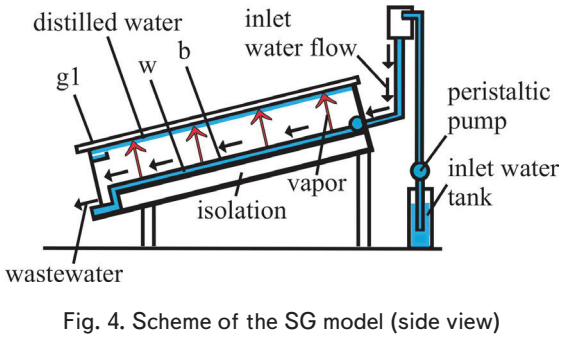

Fig. 4. Scheme of the SG model (side view)

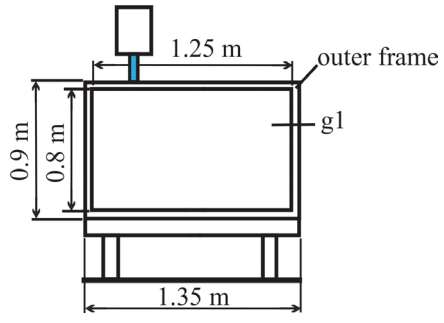

Fig. 5. Scheme of the SG model (front view)

4. 2. Mathematical model

Mathematical models for DG and SG are developed based on the energy balance of the main components with the following assumptions:

a) there is no temperature gradient between the cover glass and the absorber;

b) there is no water vapor leak;

c) condensation from water vapor on glass is uniform with negligible heat capacity;

d) the area of the absorber and the cover glass is the same;

e) the position of the cover glass is parallel to the absorber;

f) the reflection of heat radiation from dew to the absorber is ignored;

g) water flow and water temperature in the absorber are uniforms;

h) the process occurs in a steady-state.

Energy balance of DG.

Fig. 6 shows the energy balance of DG. The energy balance for the top glass (g_2), water between the top and the bottom glasses (w_f), the bottom glass (g_1), water in the absorber (w), and the wick absorber (b), respectively is:

$$\left(m\cdot C\cdot\frac{dT}{dt}\right)_{g2}=Q_{G-g2}+Q_{c,wf-g2}+$$
$$+Q_{r,g1-g2}-Q_{r,g2-a}-Q_{c,g2-a},\quad \text{watt},\qquad (1)$$

where $Q_{G\text{-}g2}$ is heat energy from lamp radiation to g_2, watt, $Q_{c,wf\text{-}g2}$ is heat energy from w_f to g_2, watt, $Q_{r,g1\text{-}g2}$ is heat energy from g_1 to g_2, watt, $Q_{r,g2\text{-}a}$ is radiation heat energy from g_2 to the surrounding, watt, and $Q_{c,g2\text{-}a}$ is convection heat energy from g_2 to the surrounding, watt.

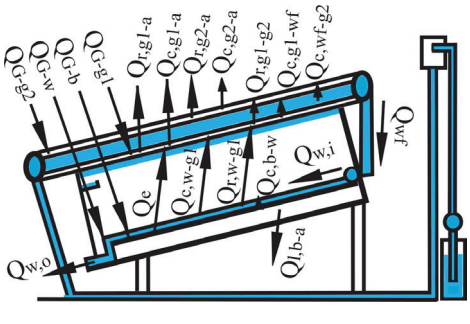

Fig. 6. Energy balance in DG

$$\left(m\cdot C\cdot\frac{dT}{dt}\right)_{wf}=Q_{wf}+Q_{c,g1-wf}-Q_{c,wf-g2},\ \text{watt},\qquad (2)$$

where Q_{wf} is heat energy from vapor condensation to w_f, watt, and $Q_{c,g1\text{-}wf}$ is heat energy from g_1 to w_f, watt.

$$\left(m\cdot C\cdot\frac{dT}{dt}\right)_{g1}=Q_{G-g1}+Q_{r,w-g1}+Q_{c,w-g1}+Q_e-$$
$$-Q_{c,g1-wf}-Q_{r,g1-g2}-Q_{r,g1-a}-Q_{c,g1-a},\quad \text{watt},\qquad (3)$$

where $Q_{G\text{-}g1}$ is heat energy from lamp radiation to g_1, watt, $Q_{r,w\text{-}g1}$ is heat energy from w to g_1, watt, $Q_{c,w\text{-}g1}$ is heat energy from w to g_1, watt, Q_e is evaporation heat, watt, $Q_{r,g1\text{-}a}$ is radiation heat energy from g_1 to the surrounding, watt, and $Q_{c,g1\text{-}a}$ is convection heat energy from g_1 to the surrounding, watt.

$$\left(m\cdot C\cdot\frac{dT}{dt}\right)_{w}=Q_{G-w}+Q_{c,b-w}+Q_{w,i}-$$
$$-Q_{r,w-g1}-Q_{c,w-g1}-Q_e-Q_{w,o},\quad \text{watt},\qquad (4)$$

where $Q_{G\text{-}w}$ is heat energy from lamp radiation to w, watt, $Q_{c,b\text{-}w}$ is heat energy from the absorber to w, watt, $Q_{w,i}$ is heat energy loss at the inlet side, watt, and $Q_{w,o}$ is heat energy loss at the exit side, watt.

$$\left(m\cdot C\cdot\frac{dT}{dt}\right)_{b}=Q_{G-b}-Q_{c,b-w}-Q_{l,b-a},\ \text{watt},\qquad (5)$$

where $Q_{G\text{-}b}$ is heat energy from lamp radiation to the absorber, watt, and $Q_{l,b\text{-}a}$ is heat energy loss from the absorber to the surrounding, watt.

Energy balance of SG.

Fig. 7 shows the energy balance of SG. The energy balance for glass (g_1), water in the absorber (w) and wick absorber (b), respectively is:

$$\left(m\cdot C\cdot\frac{dT}{dt}\right)_{g1}=Q_{G-g1}+Q_{r,w-g1}+$$
$$+Q_{c,w-g1}+Q_e-Q_{c,g1-a}-Q_{r,g1-a},\quad \text{watt};\qquad (6)$$

$$\left(m\cdot C\cdot\frac{dT}{dt}\right)_{w}=Q_{G-w}+Q_{c,b-w}+$$
$$+Q_{w,i}-Q_{r,w-g1}-Q_{c,w-g1}-Q_e-Q_{w,o},\ \text{watt};\qquad (7)$$

$$\left(m\cdot C\cdot\frac{dT}{dt}\right)_{b}=Q_{G-b}-Q_{c,b-w}-Q_{l,b-a},\ \text{watt}.\qquad (8)$$

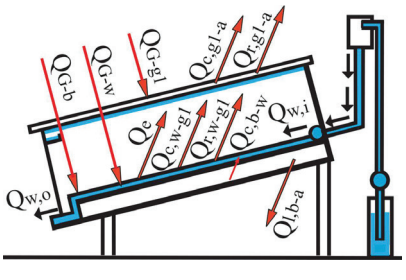

Fig. 7. Energy balance in SG

The heat energy in each part of DG and SG is

Radiation from the heating lamp to the top glass is:

$$Q_{G-g2}=G\left(1-\rho_g\right)\alpha_g A_{g2},\qquad (9)$$

where G is lamp radiation, watt, ρ_g is cover glass reflectivity, α_g is cover glass absorptivity and A_{g2} is top glass area, m^2.

Convection from water (wf) to the top glass is:

$$Q_{c,wf-g2}=A_{g2}h_w\left(T_{wf}-T_{g2}\right),\qquad (10)$$

where h_w is convection coefficient, W/m^2·°C, T_{wf} is the temperature of wf, °C, and T_{g2} is top glass temperature, °C.

Radiation from the bottom glass to the top glass is:

$$Q_{r,g1-g2} = A_{g2}h_r\left(T_{g1}-T_{g2}\right), \quad (11)$$

where h_r is radiation coefficient, W/m^2·°C, and T_{g1} is bottom glass temperature, °C.

Radiation from the top glass to the surrounding is:

$$Q_{r,g2-a} = A_{g2}h_r\left(T_{g2}-T_{sky}\right), \quad (12)$$

where T_{sky} is sky temperature, °C

Convection from the top glass to the surrounding is:

$$Q_{c,g2-a} = A_{g2}h_{wd}\left(T_{g2}-T_a\right), \quad (13)$$

where h_{wd} is wind convection coefficient, W/m^2·°C, and T_a is surrounding temperature, °C

Heat energy Q_{wf} is:

$$Q_{wf} = \dot{m}_{wi}\left(C_wT_{wf}-C_wT_{w,i}\right), \quad (14)$$

where m_{wi} is inlet water flow rate, kg/s, C_w is specific water heat, J/(kg·K), and $T_{w,i}$ is inlet water temperature, °C.

Convection from the bottom glass to water (wf) on DG is:

$$Q_{c,g1-wf} = A_{g2}h_w\left(T_{g1}-T_{wf}\right). \quad (15)$$

Radiation from the heating lamp to the bottom glass on SG and DG is:

$$Q_{G-g1} = G\left(1-\rho_g\right)\alpha_g\left[\left(A_{g1}-A_{g2}\right)+\left(1-\rho_g\right)\left(1-\alpha_g\right)A_{g2}\right], \quad (16)$$

where A_{g1} is bottom glass area, m^2

Radiation from water (w) to the bottom glass is:

$$Q_{r,w-g1} = A_bh_{r,w-g1}\left(T_w-T_{g1}\right), \quad (17)$$

where A_b is absorber area, m^2, and T_w is water temperature in the absorber, °C

Convection from water (w) to the bottom glass is:

$$Q_{c,w-g1} = A_bh_c\left(T_w-T_{g1}\right), \quad (18)$$

where h_c is convection coefficient, W/m^2·°C

Evaporation heat is:

$$Q_e = A_b.h_e.\left(T_w-T_{g1}\right), \quad (19)$$

where he is evaporation coefficient, W/m^2·°C

Radiation from the bottom glass to the surrounding on SG and DG is:

$$Q_{r,g1-a} = \left(A_{g1}-A_{g2}\right)h_{r,g1-a}\left(T_{g1}-T_{sky}\right). \quad (20)$$

Convection from the bottom glass to the surrounding on SG and DG is:

$$Q_{c,g1-a} = \left(A_{g1}-A_{g2}\right)h_{wd}\left(T_{g1}-T_a\right). \quad (21)$$

Convection from the absorber to water (w) is:

$$Q_{c,b-w} = A_bh_b\left(T_b-T_w\right), \quad (22)$$

where h_b is convection coefficient, W/m^2·°C

Radiation from the heating lamp to water (w) on SG and DG is:

$$Q_{G-w} = G\left(1-\rho_g\right)\left(1-\alpha_g\right)\alpha_w\left[\begin{matrix}\left(A_{g1}-A_{g2}\right)+\\+\left(1-\rho_g\right)\left(1-\alpha_g\right)A_{g2}\end{matrix}\right], \quad (23)$$

where α_W is water absorptivity.

Heat loss at the inlet side is:

$$Q_{w,i} = \dot{m}_{w,i}C_w\left(T_{w,i}-T_w\right). \quad (24)$$

Heat loss at the exit side is:

$$Q_{w,o} = \left(\dot{m}_{w,i}-d\dot{m}_e\right)C_w\left(T_w-T_{w,i}\right), \quad (25)$$

where dm_e is evaporation rate, kg/s.

Radiation from the heating lamp to the absorber on SG and DG is:

$$Q_{G-b} = G\left(1-\rho_g\right)\left(1-\alpha_g\right)\left(1-\alpha_w\right)\alpha_b\times \\ \times\left[\left(A_{g1}-A_{g2}\right)+\left(1-\rho_g\right)\left(1-\alpha_g\right)A_{g2}\right], \quad (26)$$

where α_b is absorber absorptivity.

Nuselt number is [15]:

$$N_u = 1+1{,}44\left[1-\frac{1708}{Ra_H\cos\theta}\right]\left[1-\frac{1708\left(sin1{,}8\theta\right)^{1{,}6}}{Ra_H\cos\theta}\right]+ \\ +\left[\left(\frac{Ra_H\cos\theta}{5830}\right)^{1/3}-1\right], \quad (27)$$

where R_{aH} is Rayleigh number, and θ is the slope of SG or DG.

Evaporation rate is: [16]

$$dme = Q_e / h_{fg}, \quad (28)$$

where h_{fg} is latent heat of water evaporation, J/kg.

Efficiency is [16]

$$\eta = \int_0^t \frac{dme\cdot h_{fg}}{A_b\cdot G}\mathrm{d}t. \quad (29)$$

The efficiency improvement of the DG model compared to the SG model was calculated for all variations of A_{g2}/A_{g1} to determine the variation in A_{g2}/A_{g1}, which results in a maximum efficiency increase. The efficiency improvement of the DG model compared to the SG in all variations of A_{g2}/A_{g1} was carried out for variations in the thickness of the cover glass of 3 mm and 5 mm.

4. 3. Experiment and simulation methods

The experiments were carried out in the Fluid Mechanics Laboratory of the University of Sanata Dharma Indonesia using heating lamps as the heat source [17]. Eight heating lamps with 400 watts per lamp are used to heat each model. Fig. 8 shows the position of the lamp. The heating lamp has a spectrum of 67 % infrared and 51 % solar radiation. The maximum average radiation on the surface of the cover glass per model that can be produced is around 1,000 watts/m^2. There is no special treatment on heating lamps to get parallel

radiation. The use of heating lamps only aims to obtain reasonable uniform radiation.

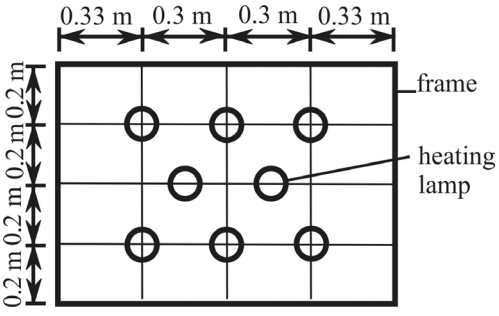

Fig. 8. Heating lamp position

The series of heating lamps are positioned parallel to the surface of the cover glass with a distance of 90 cm. The wind is simulated using three fans, which can produce a maximum wind speed of 5 m/s. Dimers and timers control heat radiation from the lamp and wind speed. The controller regulates the voltage of the heating lamp and the voltage of the motor from the fan to produce heating lamp radiation and different wind speeds every hour during the experiment. During the experiment, the heating lamp radiation was measured by a polycrystalline silicon PV cell sensor with an accuracy of 3 % (01,200 W/m^2) and a resolution of 1 W/m^2. Wind speed (V_{wd}) is measured with an anemometer.

Other data measured in the experiment are the temperature and the yield of distilled water (*dme*). Temperature data measured are ambient (T_a), cover glass (T_{g1} and T_{g2}), water in absorber (T_w), inlet water ($T_{w,i}$ for SG, and T_{wf} for DG), wastewater ($T_{w,o}$). Every temperature is measured with a DS18B20 thermocouple sensor (type K), which has a measurement range of 55 °C to +125 °C with a resolution of 0.5 °C. The DS18B20 sensor is calibrated with a standard mercury thermometer with an accuracy value of ±0.5 °C. In cover glass temperature measurement, the thermocouple is placed in the center of the cover glass. In the water in the absorber temperature measurement, the thermocouple is placed in the center of the absorber.

An e-tape liquid level sensor measured distilled water produced by each model. Measurement data from all sensors are recorded using an Arduino microcontroller data logger that has been programmed to record each sensor's data every 1 minute. The microcontroller used is Seeeduino Stalker v2 (ATMEGA328). The microcontroller is connected to a PC wirelessly using a wireless sensor node and Wi-Fi to monitor the sensor's data. The experiment begins by regulating the same mass flow of inlet water of 3.5 kg/hour in the DG and SG models. A small 5W peristaltic pump was used to maintain a constant flow of the inlet water. The inlet water mass flow of 3.5 kg/hour was carried out for 10 hours for each variation.

A simulation was made based on the mathematical model. The temperature of each main component and the distilled water produced from DG and SG can be calculated. Calculations are carried out by the Euler method numerically to solve first-order differential equations simultaneously from DG and SG. The simulation is done using TrnSys software [18]. The integration of the DG and SG models into the TrnSys software is done using a FORTRAN program.

5. Results

5. 1. Comparison of distilled water results from experiments and simulations

The first stage of this research is the experiments in the laboratory. Experiments were carried out on both SG and DG models. The thickness of the cover glass used is 3 mm.

Fig. 9 shows the ambient air temperature and wind speed during the experiment.

Fig. 10 shows the heat radiation from the heating lamp during the 10hour test.

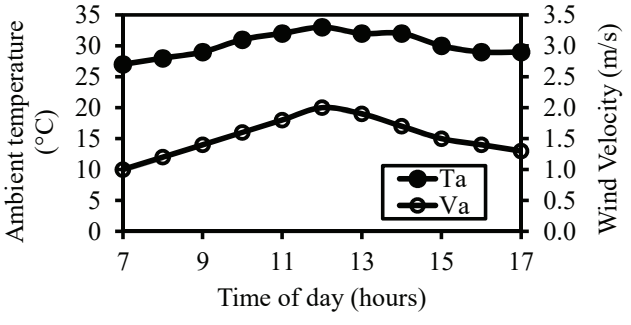

Fig. 9. Average ambient temperature and wind velocity during the experiment

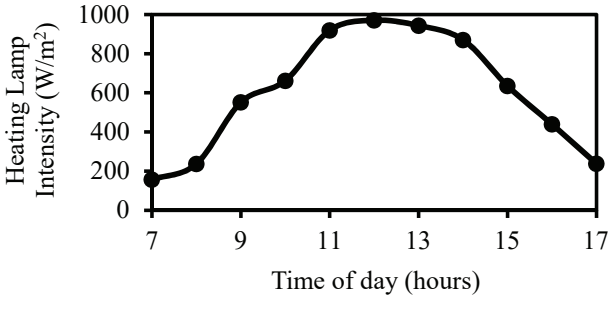

Fig. 10. Average irradiance of the heating lamp during the experiment

The second step is to simulate both SG and DG models. The simulations are carried out using the same ambient air temperature, wind speed, and heat radiation data as the experiments. The thickness of the cover glass of both the SG and DG models used in the simulation is also 3 mm.

Fig. 11 shows a comparison of distillation water results from experiments and simulations for the A_{g2}/A_{g1} ratio of 0.0, 0.1, 0.5, 0.7, and 1.0. As can be seen from the graph, the difference in distillation water results from experiments and simulations ranges from 1.70 % to 4.8 %. The difference in temperature of the SG and DG models from experiments and simulations ranges within 2—3 °C. Differences in the results of distillation water and temperature in that range are commonly obtained in similar studies [11, 12, 17]. As well as showing the simulation results are valid.

Fig. 11 shows that the distilled water produced by the DG model is more than the SG model for all variations of the A_{g2}/A_{g1} ratio. However, Fig. 11 also shows that the higher the ratio of A_{g2}/A_{g1}, the less distilled water is produced by the DG distillation model. In other words, the greater the A_{g2}/A_{g1} ratio, the smaller the efficiency improvement of the DG model compared to the efficiency of the SG model.

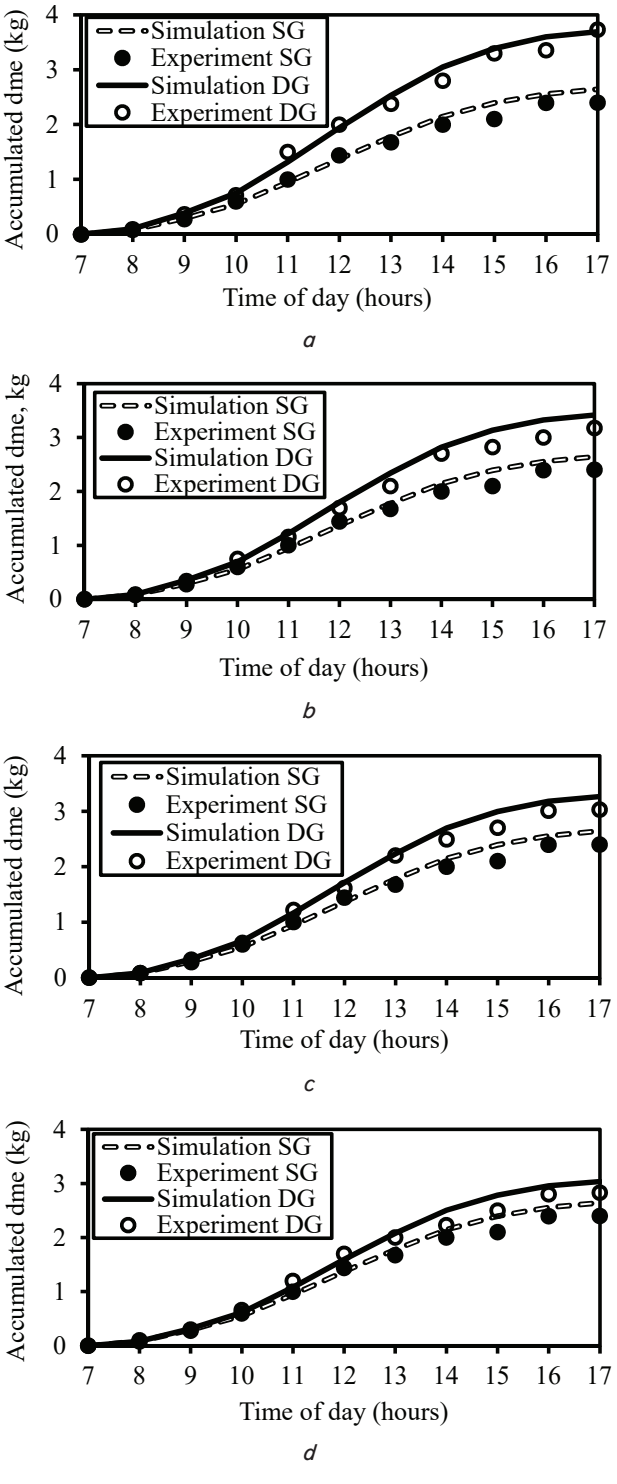

Fig. 11. Comparison of distillation water results from experiments and simulations on the SG and DG models with the 3 mm thick cover glass: *a* – DG with A_{g2}/A_{g1}=0.1, *b* – DG with A_{g2}/A_{g1}=0.5, *c* – DG with A_{g2}/A_{g1}=0.7, *d* – DG with A_{g2}/A_{g1}=1.0

5. 2. Effects of heat recovery using double glass on distillation efficiency

The first and second stages of this study showed the results of the simulation carried out following the results of the experiment. The third stage of this research is to conduct a simulation like the second stage, but the thickness of the cover glass used by both the SG and DG models is 5 mm. The results of the second and third stage simulations in the two models were compared to analyze the effects of heat recovery using double glazing on the efficiency of distillation. Fig. 12 shows the results of the distillation water of both SG and DG models using 3 mm and 5 mm cover glass thickness. SG is the distillation model with A_{g2}/A_{g1} of 0. DG is ~~is~~ the distillation model with A_{g2}/A_{g1} of 0.1, 0.5, 0.7, and 1.0.

As shown in Fig. 12, the distillation water produced by both the SG and DG models with the 3 mm cover glass is on average 58.9 % more than the distillation water produced by both models with the 5 mm cover glass. On the variation of the thickness of the 3 mm cover glass, the DG model with A_{g2}/A_{g1} of 0.1, 0.5, 0.7, and 1.0 produced more distilled water than the SG model. On the variation of the thickness of the 5 mm cover glass, the DG model with A_{g2}/A_{g1} of 0.1, 0.5, and 0.7 produced more distilled water than the SG model. However, on A_{g2}/A_{g1} of 1.0, the DG model produced distilled

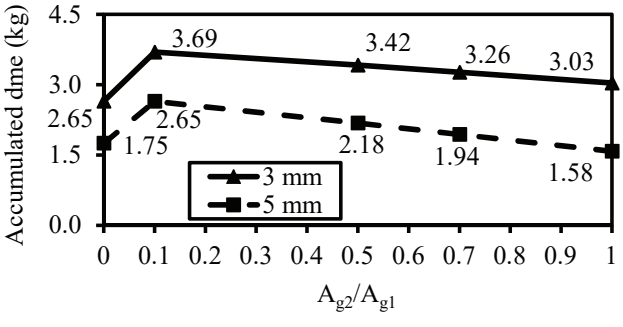

Fig. 12. Yield of distilled water per day

water less than SG.

The resulting distillation water is directly proportional to the distillation efficiency. As shown in Fig. 13, the efficiency produced by both the SG and DG models on the 3 mm thick cover glass variation is higher than the efficiency of the two models on the 5 mm thick cover glass variation. On the variation of the thickness of the 3 mm cover glass, the DG model efficiency with A_{g2}/A_{g1} of 0.1, 0.5, 0.7, and 1.0 is higher than the efficiency of the SG model. On the 5 mm thick cover glass variation, the efficiency of the DG model with A_{g2}/A_{g1} of 0.1, 0.5, and 0.7 is higher than the SG model. However, on the A_{g2}/A_{g1} of 1.0, the efficiency of the DG model is lower than the efficiency of the SG model.

Fig. 14 shows an increase in the efficiency in both the SG and DG distillation models against the SG model as a comparison. Increased efficiency is the difference between the efficiency of the model and the efficiency of the SG model divided by the efficiency of the SG model.

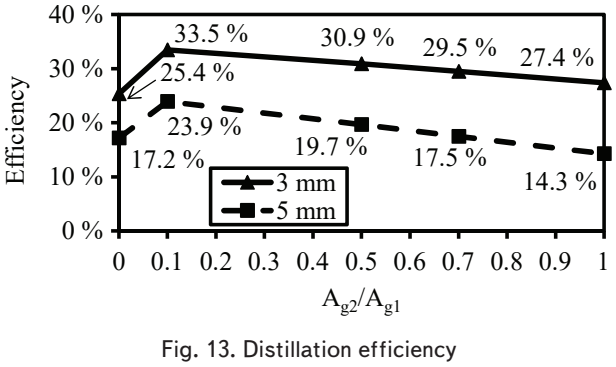

Fig. 13. Distillation efficiency

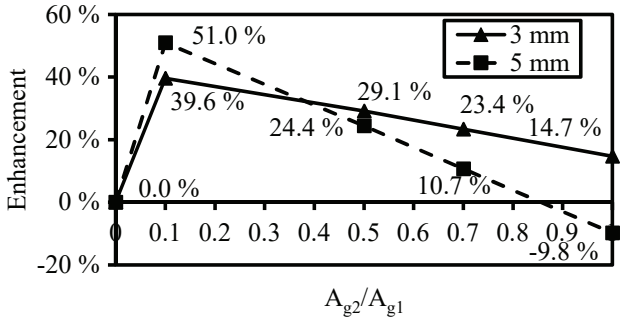

Fig. 14. Enhancement of distillation efficiency against the SG model

As can be seen in Fig. 14, on the cover glass of 3 mm thickness, the increase in the efficiency of the DG model with A_{g2}/A_{g1} of 0.1, 0.5, 0.7, 1.0 is positive. A positive value of increasing efficiency shows that in the 3 mm thick cover glass variation, the DG model efficiency is higher than the SG model for all A_{g2}/A_{g1} values. In the 5 mm thick cover glass variation, the increase in the efficiency of the DG model with A_{g2}/A_{g1} of 1.0 is negative. A negative value indicates that at the same top glass area as the bottom glass, the DG model distillation efficiency is lower than the SG model.

Fig. 15 shows the temperature of the water entering into both the SG and DG distillation models. In the SG model, inlet water comes from the water reservoir and directly enters the SG model, without preheating. Water that enters the DG model gets preheated so that the temperature of the water entering the DG model is higher than that of the water entering the SG model. Before water enters the DG model, water flows between the top and bottom glass. During flow between the top glass and the bottom glass, water gets heat energy from the bottom glass. The heat from the bottom glass that moves to water comes from water vapor that releases heat to the bottom glass when condensing. The utilization of condensing heat to heat distilled input water is called the heat recovery process. The temperature of water entered into the DG model at 3 mm thick cover glass variation is higher than in the 5 mm thick cover glass variation. Higher inlet water temperature indicates more moisture that is condensed so that the condensation heat is received more by the water.

Fig. 16 shows the amount of condensation heat received by water (Q_{wf}) before entering the distillation model. As shown in the graph, the condensation heat received by water (Q_{wf}) before entering the DG model at 3 mm glass thickness variation is on average 12.7 % greater than the 5 mm glass thickness variation.

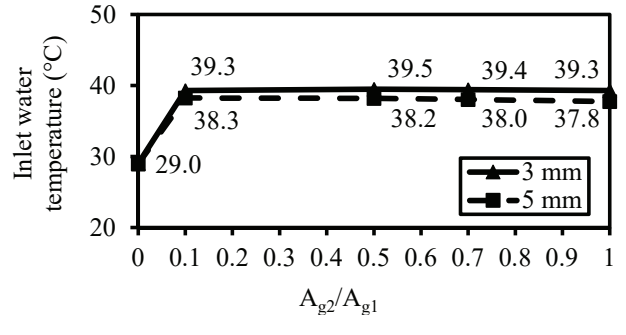

Fig. 15. Inlet water temperature

DG model distillation has advantages over the SG model because, in the DG model, the heat recovery process can be carried out so that the inlet water temperature is higher than in the SG model. However, the use of double glazing in the DG model to carry out the heat recovery process has disadvantages. The use of double glazing in the DG model causes less heat radiation to be received by the absorber compared to the SG model distillation, which uses only one cover glass. The heat radiation that comes in the distillation model always passes through the cover glass before the absorber is received. Not all heat radiation received by the cover glass is transmitted to the absorber. Some of the heat radiation is reflected in the environment, and the cover glass absorbs some. In the SG model distillation, which only has one glass cover, the heat radiation received by the glass cover is reflected and absorbed once. In the DG model distillation, which has two glass covers, the incoming heat radiation is reflected and absorbed twice. The greater the area of the top cover glass, the more heat radiation is reflected and absorbed by the cover glass. The more heat radiation reflected and absorbed by the cover glass, the less heat radiation the absorber receives. As an illustration, in the DG model distillation with A_{g2}/A_{g1} of 0.1 (Fig. 17), the top glass and the bottom glass reflected and absorbed 10 % of the heat radiation. At the same time, 90 % of the thermal radiation is reflected and absorbed by the bottom glass. The thickness of the glass also affects the amount of heat radiation reflected and absorbed by the cover glass. The thicker the cover glass, the greater the reflectivity and absorbance value of the glass. In other words, the thicker the cover glass, the more heat radiation is reflected and absorbed by the cover glass. Fig. 18 shows the heat radiation received by the absorber on both the SG and DG distillation models.

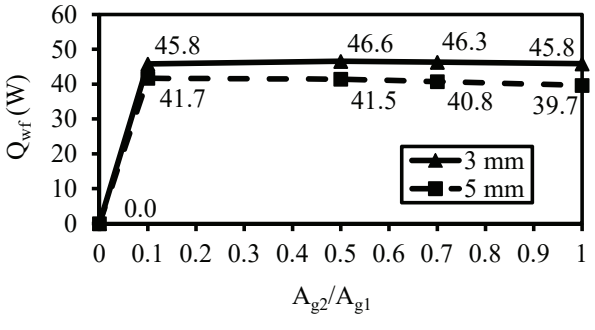

Fig. 16. Amount of condensation heat received by water (Q_{wf})

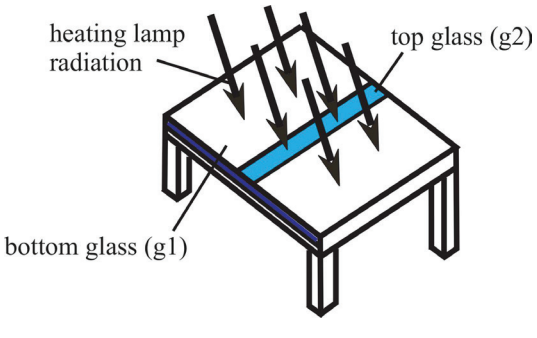

Fig. 17. Heat radiation on the DG model with A_{g2}/A_{g1} of 0.1

As shown in the graph, the heat radiation received by the absorber on both models with a 3 mm cover glass thickness is, on average, 37.7 % greater than with the 5 mm cover glass thickness. Fig. 18 also shows that the higher the A_{g2}/A_{g1} value, the less heat radiation the absorber receives.

The heat radiation received by the absorber and the inlet water temperature affect the temperature of the water

in the absorber. Fig. 19 shows the water temperature in the absorber of both SG and DG models in the variation of the thickness of the cover glass 3 mm and 5 mm. It is clear from the chart that the water temperature on the model absorber with the 3 mm thick glass cover is, on average 5.6 % higher than the water temperature of the model with the 5 mm thick glass cover.

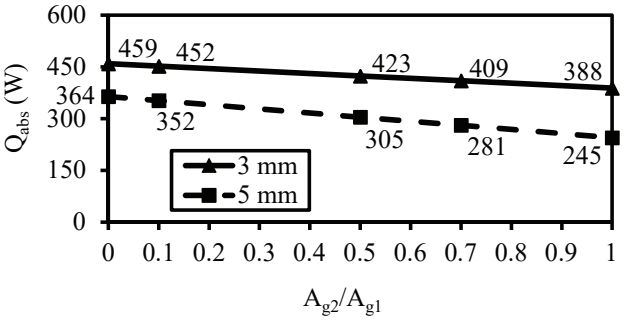

Fig. 18. Heat radiation received by the absorber

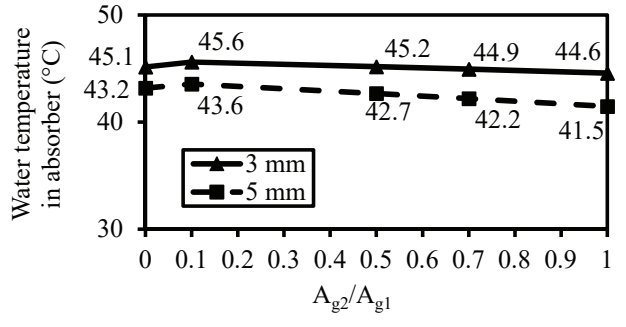

Fig. 19. Water temperature in the absorber

Fig. 19 shows that the water temperature in the absorber from the DG model distillation with A_{g2}/A_{g1} of 0.1 and 0.5 is higher than for the SG model. However, the water temperature in the absorber from the DG model distillation with $A_{g2}/A_{g1}$of 0.7 and 1.0 is lower than from the SG model distillation. The water temperature at the absorber from the DG model distillation with the 5 mm thick glass cover is higher than the water temperature at the absorber from the SG model only at the A_{g2}/A_{g1} value of 0.1.

The temperature of the cover glass is influenced by the heat radiation absorbed by the cover glass and the condensation heat of water vapor received by the cover glass. In the DG model, water vapor condenses on the inner surface of the bottom cover glass. The more water vapor that condenses, the higher the bottom cover glass temperature.

Fig. 20 shows that the temperature of the bottom cover glass of the DG model with the 5 mm thick glass is 3.5 % lower than the temperature of the bottom cover glass of the DG model with the 3 mm thick glass. The temperature of the DG glass cover model with the 5 mm thick glass is lower due to less distilled water produced, meaning that water vapor is also condensed less. The weight of the 5 mm thickness cover glass is greater than the weight of the 3 mm thickness cover glass. The greater mass of the glass causes the heat capacity of the 5 mm thick cover glass greater than the heat capacity of the 3 mm thick cover glass. The higher the heat capacity of the cover glass, the lower the cover glass temperature.

As it has been explained above, distilled water from the DG model with the 3 mm thick cover glass is more than SG models distilled water. More distilled water shows more water vapor that condenses on the inner surface of the bottom cover glass. The more water vapor that condenses, the more heat receives by the cover glass. In other words, the temperature of the bottom cover glass of the DG model should be higher than the temperature of the cover glass of the SG model.

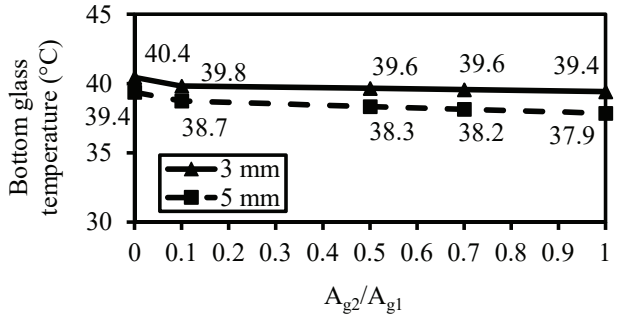

Fig. 20. Bottom glass temperature

Fig. 20 precisely shows the opposite. The DG glass cover temperature is lower than the SG glass cover temperature. The temperature of the DG glass cover is lower than the SG cover glass temperature, which shows that the inlet water flow between the top glass and the bottom glass also functions as cover glass cooling water.

Water vapor in the SG and DG distillation models moves from the absorber to the surface of the inner cover glass and then condenses. The water vapor movement is strongly influenced by the temperature difference between the water temperature in the absorber and the temperature of the bottom cover glass (ΔT). The higher the value ΔT, the faster the water vapor moves from the absorber surface to the inner surface of the cover glass. Fig. 21 shows the ΔT values of the SG and DG models. It can be seen from the graph that (ΔT) of both models with the 3 mm thick glass cover is higher than the ΔT value of both models with the 5 mm thick glass cover. On the 3 mm thick cover glass variation, the ΔT value of the DG distillation model with A_{g2}/A_{g1} of 0.1, 0.5, 0.7, and 1.0 is higher than the ΔT value of the SG distillation model. On the 5 mm thick cover glass variation, the ΔT value of the DG distillation model with A_{g2}/A_{g1} of 1.0 is lower than the ΔT value of the SG distillation model. The lower value of ΔT causes less distillation water produced by the DG model with A_{g2}/A_{g1} of 1.0 than by the SG model distillation.

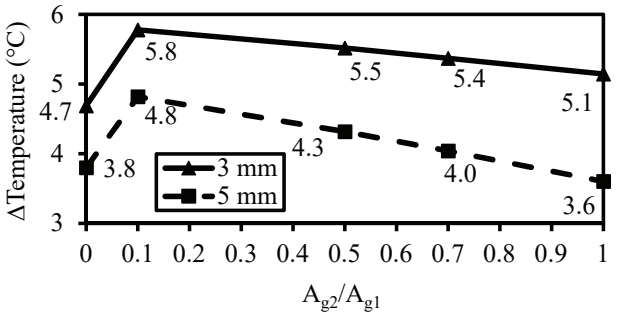

Fig. 21. Temperature difference between the water temperature in the absorber and the temperature of the bottom cover glass

Fig. 21 also shows that the DG distillation model with the A_{g2}/A_{g1} value increases; the value of ΔT decreases. The decreasing ΔT value is caused by the heat radiation received

by the absorber decreases at a higher A_{g2}/A_{g1} value. The greater A_{g2}/A_{g1} value causes more heat radiation to be reflected and absorbed by the glass.

The transfer of water vapor from the absorber to the inner surface of the cover glass is also affected by the evaporative heat transfer coefficient. The convection heat transfer coefficient influences the evaporative heat transfer coefficient. Fig. 22 and Fig. 23 show that the convection heat transfer coefficient and the evaporative heat transfer coefficient of the DG model are on average 13.5 % and 24.1 % higher than those of the SG model, respectively.

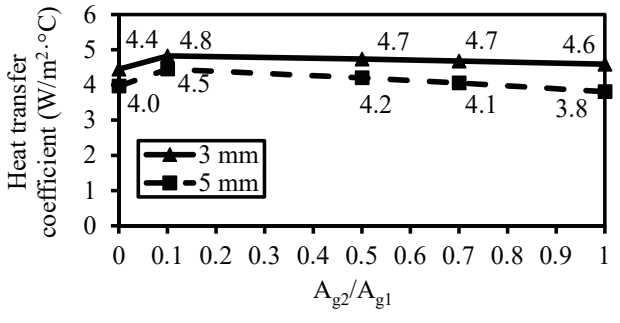

Fig. 22. Convection heat transfer coefficient

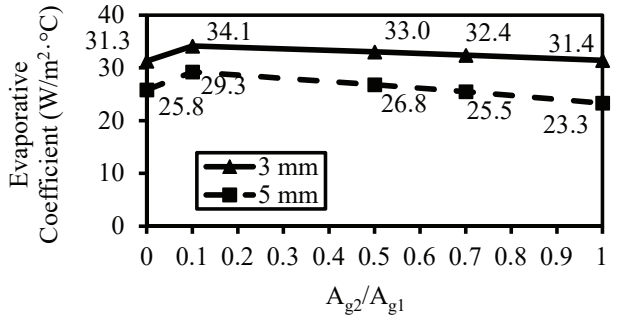

Fig. 23. Evaporative heat transfer coefficient

In the SG and DG distillation models, heat energy losses occur during the distillation process. Heat energy losses that occur include heat energy losses at the inlet and exit sides. The loss of heat energy at the inlet is caused by the temperature of the water entering the distillation model. The inlet water has a lower temperature than the temperature of the water at the absorber. The lower the temperature of the inlet water, the higher the loss of heat energy at the inlet side.

After the water enters the distillation model, water flows on the surface of the absorber. During flow on the surface of the absorber, water gets heat energy from the absorber by convection. While flowing, some of the water evaporates and condenses on the inner surface of the cover glass. Some cannot evaporate and comes out of the distillation model from the exit side as hot water. Hot water that comes out on the exit side of the distillation model is a loss of heat on the exit side. The more water that does not evaporate and comes out, the higher the loss of heat energy that occurs on the exit side. Fig. 24, 25 show the heat energy losses at the inlet and exit sides of both the SG and DG distillation models. As shown in the graph, the heat energy losses at the inlet and exit sides of the two models with the 3 mm thick glass cover are higher than with the 5 mm glass cover.

The heat loss at the inlet side is influenced by the flow rate of the inlet water and the difference between the absorber temperature and the inlet water temperature. The flow rate of the inlet water in all models is the same. In other words, the heat loss at the inlet side is greater in the model with the 3 mm cover glass due to the greater difference between the absorber temperature and the intake water temperature.

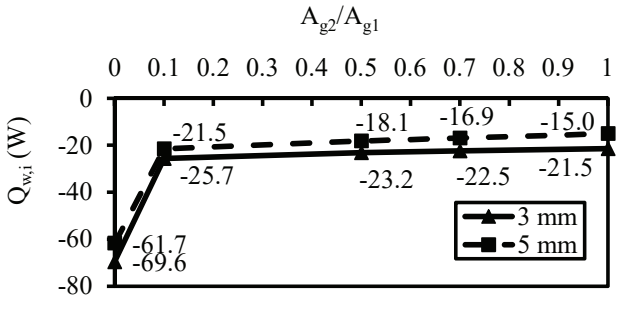

Fig. 24. Heat energy losses at the inlet side

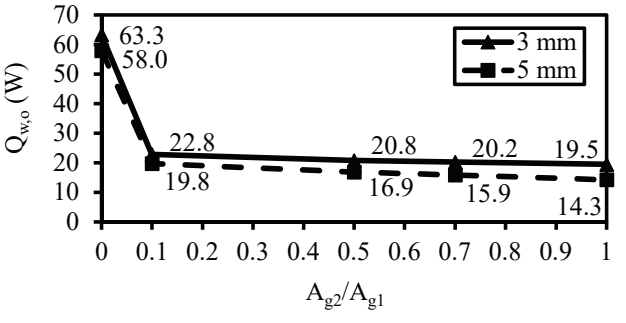

Fig. 25. Heat energy losses at the exit side

The heat loss on the exit side is influenced by the flow rate of the water that does not evaporate, and the temperature difference between the absorber and the inlet water temperature. The non-evaporating water flow rate on the model with the 3 mm cover glass is less than on the model with the 5 mm cover glass. In other words, the higher exit side heat loss on the model with the 3 mm cover glass is also due to the greater difference between the absorber temperature and the intake water temperature.

6. Discussion of experimental results

The results of the research described above show that the heat recovery process using double glazing can increase the yield of distilled water and distillation efficiency. The increase in water yield and distillation efficiency can be seen from the comparison of the results of distillation water and the efficiency of the distillation model with heat recovery, i.e. the DG model compared to the SG distillation model that does not use the heat recovery process.

Fig. 12, 13 show the comparison of distillation water yield and DG model distillation efficiency compared to SG model distillation with the 3 mm and 5 mm thick glass cover on A_{g2}/A_{g1} variations of 0.1, 0.5, 0.7, and 1.0. The maximum efficiency increase of DG compared to SG was achieved in the A_{g2}/A_{g1} variation of 0.1. The maximum efficiency increase of DG compared to SG with the cover glass thickness of 3 mm is 39.6 % and 51.0 % with the cover glass thickness of 5 mm (Fig. 14). More distillation water yields and higher efficiency from DG model distillation compared to SG model distillation are due to the inlet water temperature of

the DG distillation model, which is higher 9.7 ϵC or 33.5 % than the SG model distillation water temperature (Fig. 15). Heat recovery in the DG model distillation causes the higher temperature of the water entering the DG model distillation than the temperature of the SG model distillation inlet water. Heat recovery also causes DG model distillation to get heat energy carried by water into the absorber of Q_{wf} (Fig. 16). The only disadvantage of using double glazing to carry out the heat recovery process is the reduced heat energy received by the absorber. In other words, the use of double glass causes the heat energy received by the absorber to DG model distillation to be less than the SG model distillation, which uses only a single glass (Fig. 18). Heat recovery using double glazing on DG distillation models results in the cooling effect of glass by entering water flowing in the channel between the bottom glass and the top glass. Cooling of the glass by inlet water causes the temperature of the cover glass in the DG model distillation to be lower than the temperature of the cover glass on the SG model (Fig. 20). Furthermore, lower glass temperatures cause the difference in water temperature at the absorber with the cover glass temperature (ΔT) in the DG model distillation higher than ΔT in the SG model distillation (Fig. 21). In addition to causing higher ΔT, heat recovery also causes the evaporative heat transfer coefficient of the DG model distillation to be higher than the SG model distillation (Fig. 23). Heat recovery also reduces heat loss at the inlet side (Fig. 24). The reduction in heat energy losses at the inlet side of DG is 45.1 W or 68.7 % compared to SG. Higher ΔT and higher evaporative heat transfer coefficient and less heat energy losses at the inlet side cause the water in the absorber to evaporate faster. The temperature of the water in the absorber (Fig. 19) shows the temperature when the water undergoes a process of evaporation. In Fig. 19, the actual temperature of water in the absorber from the DG model distillation and the SD model distillation is not much different. However, the higher inlet water temperature in the DG model distillation compared to the SG model causes the water evaporation temperature in the DG distillation model to be achieved in a faster time than in the SG distillation model. The more rapid evaporation temperature achieved by water in the absorber from the DG model distillation causes the evaporation process time of the water to the absorber to be longer. Fig. 26 shows the distance needed for the inlet water to reach the evaporation temperature from the inlet side (L_h) and the length of the water at the absorber for the evaporation process (L_e).

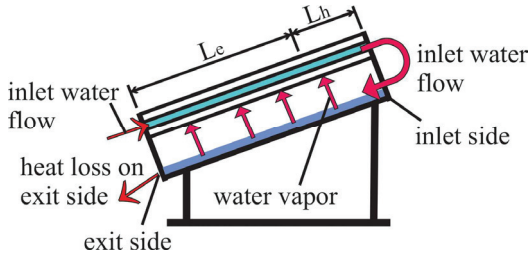

Fig. 26. Distance to reach the evaporation temperature and process

The lower the inlet water temperature, the longer the L_h distance. The longer the L_h distance, the longer the time it takes for water to reach the evaporation temperature. The greater length of L_h causes a shorter length of L_e. The shorter the L_e distance, the less time is needed for the water in the absorber to evaporate. The short time of evaporation causes less amount of water to evaporate. The less water evaporating in the absorber causes less yield of distilled water. The less water evaporating in the absorber causes the water in the absorber that does not evaporate and comes out as hot water on the exit side more and more. In other words, the loss of heat energy on the exit side is greater. The longer evaporation process causes the distillation water produced by DG model distillation to be higher than the distillation water produced by the SG model distillation. The evaporation temperature of water in the absorber of the SG model is achieved in a longer time than DG. So the process of evaporation of water at the absorber only has a short time. The shorter time for the process evaporation of water at the absorber causes a lot of water that has not enough time to evaporate and come out of the distillation model as hot water. The loss of heat energy on the exit side from the DG model distillation is about 41.9W or 69.1 % lower than that of the SG model distillation, showing that the mass of water that has no time to evaporate and exit the DG distillation model is less than that of the SG model distillation. In other words, the distillation water produced by the SG distillation model is less than the DG model distillation. The time required for the inlet water of the SG and DG distillation models to reach the evaporation temperature is influenced by the temperature of the water when entering the distillation model and the heat energy received by the water from the absorber. The heat energy received by the water from the absorber is influenced by the heat energy received by the absorber from heat radiation and energy losses at the inlet side. It has been said that the heat recovery process causes the temperature of water to enter the DG distillation model on the 3 mm and 5 mm cover thickness variation and A_{g2}/A_{g1} of 0.1, 0.5, 0.7 and 1.0 to be higher than the temperature of the water entering the SG distillation model. The maximum heat energy received by water entering the distillation model from the absorber is equal to the difference from the heat energy received by the absorber from heat radiation with losses at the inlet side (Fig. 27).

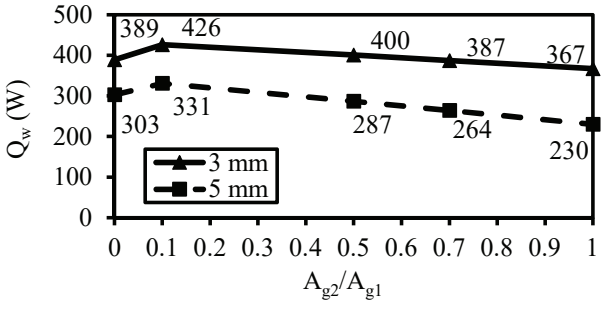

Fig. 27. Heat energy received by inlet water from the absorber

Fig. 27 shows the variation of the thickness of the 3 mm cover glass and the A_{g2}/A_{g1} values of 0.1 and 0.5, the heat energy received by the water from the absorber on the DG model distillation is higher than on the SG model distillation. Higher inlet water temperatures and heat energy received by water from the absorber, which is higher in DG distillation models with the 3 mm thick glass cover and A_{g2}/A_{g1} of 0.1 and 0.5, cause water evaporation temperature to be achieved faster than in the distillation of the SG model. The evaporation temperature completed more quickly causes the evaporation time to be longer so that the DG model with the 3 mm thick

glass cover and A_{g2}/A_{g1} of 0.1 and 0.5 produces more distilled water than the SG model distillation.

The same thing happened with the 5 mm thick cover glass variation. However, in the 5 mm thick cover glass variation, the heat energy received by the DG model is higher than by the SG model, occurring only at A_{g2}/A_{g1} values of 0.1.

The heat energy received by water from the absorber on the DG model with the 3 mm thick glass cover and A_{g2}/A_{g1} values of 0.7 and 1.0 is less than in the distillation of the SG model. Even though the heat energy received by the water from the absorber is lower, the evaporation temperature is still achieved in a faster time, due to the higher inlet water temperature. The more rapid evaporation temperature reached causes the evaporation time to be longer so that the distillation water from the DG model with the 3 mm thick cover glass and A_{g2}/A_{g1} of 0.7 and 1.0 is still higher than in the distillation of the SG model.

The same thing happened with the variation of 5 mm thick cover glass with A_{g2}/A_{g1} values of 0.5 and 0.7. In the 5 mm thick cover glass variation and A_{g2}/A_{g1} values of 0.5 and 0.7, the heat energy received by water from the absorber on the DG model distillation is 19.7 % lower than on the SG model distillation.

In the 5 mm thick cover glass variation and A_{g2}/A_{g1} value of 1.0, the heat energy received by water from the absorber in the DG model distillation is 32.8 % lower than in the SG model distillation. Even though the inlet water temperature is higher, because the heat energy received by the water from the absorber is very low, the evaporation temperature is still achieved for a longer time. The longer time for evaporation temperature reached causes less time for evaporation so that the resulting distillation water from the DG model with the 5 mm thick glass cover and A_{g2}/A_{g1} of 1.0 is less than in the SG model distillation.

The results of the research, as described above, show that the use of heat recovery using double glazing can increase the temperature of the intake water more efficiently and cheaply than previous studies. Increasing the inlet water temperature causes reduced heat losses on the inlet and outlet sides. The reduced heat loss improves the distillation efficiency.

The increase in intake water temperature is output, and an increase in efficiency is the proposed design outcome. The results showed that the temperature increase reached an average of 33.5 %. The increase in efficiency was achieved by an average of 39.6 % (using the 3 mm thick glass) and 51 % (using the 5 mm thick glass). Effectiveness is the ratio between outcome and output. The effectiveness value of the proposed design was more than one. In other words, the proposed design is effective. However, the effectiveness needs to be tested by experiment in real field conditions for a long time. For example, decreased absorber absorption due to distilled water contaminants' deposition due to long use times also affects the proposed design's effectiveness.

Compared to previous studies, the proposed method has the advantage of being more straightforward and cheaper. The increase in efficiency resulting from the proposed method is also better than previous studies. As a comparison, the increase in distillation efficiency using a solar water collector [8] was 36 %. With the proposed method, the maximum efficiency increase that could be achieved was 39.6 %.

The limitation of this study is that this method is suitable only for the distillation of seawater or water contaminated with small contaminants. Large contaminants such as soil are not ideal for the proposed model because large contaminants can clog the drain gaps in double glazing.

The disadvantage of this method is that the maximum efficiency increase occurs in the A_{g2}/A_{g1} variation of 0.1, meaning that only 10 % of the condensation heat is utilized. In the future, research is needed to find methods that can make maximum use of the heat of condensation.

This study can be developed further to reduce more heat energy losses on the inlet and exit sides. The difficulties that may be encountered are related to the development of a suitable mathematical model. Another possible difficulty is technical issues for experimental testing.

7. Conclusions

1. The average increase in the inlet water temperature of the DG model was 33.5 % compared to the temperature of the inlet water of the SG model.

2. The reduction in heat energy losses of the DG model compared to the SG model at the inlet side and exit side was 68.7 % and 69.1 %, respectively.

3. Heat recovery improves distillation efficiency. The maximum efficiency improvement of the DG model compared to SG models of 39.6 % and 51.0 % were achieved with the 3 mm and 5 mm thick cover glasses, respectively.

4. The maximum efficiency of the DG model was achieved at A_{g2}/A_{g1} variations of 0.1.

Acknowledgments

The author is grateful for the financial support from the Directorate General of Higher Education of the Republic of Indonesia.

References

1. Omara, Z. M., Kabeel, A. E., Abdullah, A. S. (2017). A review of solar still performance with reflectors. Renewable and Sustainable Energy Reviews, 68, 638–649. doi: https://doi.org/10.1016/j.rser.2016.10.031
2. Hansen, R. S., Narayanan, C. S., Murugavel, K. K. (2015). Performance analysis on inclined solar still with different new wick materials and wire mesh. Desalination, 358, 1–8. doi: https://doi.org/10.1016/j.desal.2014.12.006
3. Das, D., Bordoloi, U., Kalita, P., Boehm, R. F., Kamble, A. D. (2020). Solar still distillate enhancement techniques and recent developments. Groundwater for Sustainable Development, 10, 100360. doi: https://doi.org/10.1016/j.gsd.2020.100360
4. Muthu Manokar, A., Kalidasa Murugavel, K., Esakkimuthu, G. (2014). Different parameters affecting the rate of evaporation and condensation on passive solar still – A review. Renewable and Sustainable Energy Reviews, 38, 309–322. doi: https://doi.org/10.1016/j.rser.2014.05.092
5. Prakash, P., Velmurugan, V. (2015). Parameters influencing the productivity of solar stills – A review. Renewable and Sustainable Energy Reviews, 49, 585–609. doi: https://doi.org/10.1016/j.rser.2015.04.136

6. Nagarajan, P. K., El-Agouz, S. A., Harris Samuel, D. G., Edwin, M., Madhu, B., Magesh babu, D. et. al. (2017). Analysis of an inclined solar still with baffles for improving the yield of fresh water. Process Safety and Environmental Protection, 105, 326–337. doi: https://doi.org/10.1016/j.psep.2016.11.018
7. Sharon, H., Reddy, K. S., Krithika, D., Philip, L. (2017). Experimental performance investigation of tilted solar still with basin and wick for distillate quality and enviro-economic aspects. Desalination, 410, 30–54. doi: https://doi.org/10.1016/j.desal.2017.01.035
8. Sathyamurthy, R., El-Agouz, S. A., Nagarajan, P. K., Subramani, J., Arunkumar, T., Mageshbabu, D. et. al. (2017). A Review of integrating solar collectors to solar still. Renewable and Sustainable Energy Reviews, 77, 1069–1097. doi: https://doi.org/10.1016/j.rser.2016.11.223
9. Abdullah, A. S., Essa, F. A., Omara, Z. M., Bek, M. A. (2018). Performance evaluation of a humidification–dehumidification unit integrated with wick solar stills under different operating conditions. Desalination, 441, 52–61. doi: https://doi.org/10.1016/j.desal.2018.04.024
10. Sharshir, S. W., El-Samadony, M. O. A., Peng, G., Yang, N., Essa, F. A., Hamed, M. H., Kabeel, A. E. (2016). Performance enhancement of wick solar still using rejected water from humidification-dehumidification unit and film cooling. Applied Thermal Engineering, 108, 1268–1278. doi: https://doi.org/10.1016/j.applthermaleng.2016.07.179
11. Kabeel, A. E., Taamneh, Y., Sathyamurthy, R., Naveen Kumar, P., Manokar, A. M., Arunkumar, T. (2018). Experimental study on conventional solar still integrated with inclined solar still under different water depth. Heat Transfer-Asian Research, 48 (1), 100–114. doi: https://doi.org/10.1002/htj.21370
12. Samuel Hansen, R., Kalidasa Murugavel, K. (2017). Enhancement of integrated solar still using different new absorber configurations: An experimental approach. Desalination, 422, 59–67. doi: https://doi.org/10.1016/j.desal.2017.08.015
13. El-Agouz, S. A., El-Samadony, Y. A. F., Kabeel, A. E. (2015). Performance evaluation of a continuous flow inclined solar still desalination system. Energy Conversion and Management, 101, 606–615. doi: https://doi.org/10.1016/j.enconman.2015.05.069
14. Shekarchi, N., Shahnia, F. (2018). A comprehensive review of solar-driven desalination technologies for off-grid greenhouses. International Journal of Energy Research, 43 (4), 1357–1386. doi: https://doi.org/10.1002/er.4268
15. Hollands, K. G. T., Unny, T. E., Raithby, G. D., Konicek, L. (1976). Free Convective Heat Transfer Across Inclined Air Layers. Journal of Heat Transfer, 98 (2), 189–193. doi: https://doi.org/10.1115/1.3450517
16. Duffie, J. A., Beckman, W. A. (1991). Solar engineering of thermal processes. Wiley.
17. Mahdi, J. T., Smith, B. E., Sharif, A. O. (2011). An experimental wick-type solar still system: Design and construction. Desalination, 267 (2-3), 233–238. doi: https://doi.org/10.1016/j.desal.2010.09.032
18. Raza, H. A., Sultan, S., Shomaz-Ul-Haq, Ali, M. (2018). Modelling of efficient solar water desalination\system using TRNSYS. 2018 International Conference on Engineering and Emerging Technologies (ICEET). doi: https://doi.org/10.1109/iceet1.2018.8338622
19. Tanaka, H. (2017). Parametric investigation of a vertical multiple-effect diffusion solar still coupled with a tilted wick still. Desalination, 408, 119–126. doi: https://doi.org/10.1016/j.desal.2017.01.019